PIER Letters

(Received 27 February 2023, Accepted 10 January 2024, Scheduled 31 January 2024)

Curvature-Based Feature Representation for Ship Detection in SAR Image

Zhenyu Chen and Meng Yang*

Hangzhou Dianzi University, Hangzhou, China

ABSTRACT: This article aims to exploit Ricci tensor with certain geometric properties which are used for feature representation and ship detection in synthetic aperture radar (SAR) image. The proposed method is composed of the following key points. Firstly, Riemannian metrics on the Gamma manifold are constructed based on the family of Gamma density functions. Secondly, direct calculation gives the Ricci tensor of Gamma manifold, where the curvature tensor resorts to the torsion-free affine connection. Thirdly, a general scheme for Zermelo navigation problem on the Riemannian manifold is addressed, and the solution of the navigation problem is proposed. Fourthly, feature representation problems are formulated as certain forms of Finsler metric of Randers type, indicating a joint framework for extracting low-dimensional features with closed-form solutions. Comprehensive experiments on real SAR image data sets demonstrate the effectiveness of the proposed method against compared state-of-the-art detection approaches.

1. INTRODUCTION

Synthetic aperture radar (SAR) which is a high resolution coherent radar is a significant space remote sensing method and has evolved to satisfy a variety of applications for both civilian and military users. Among these applications, researches of ship detection using SAR images have received considerable attention in the area of marine remote sensing [1].

As a coherent imaging system, SAR images contain lots of speckle noise. The researches show that the sea clutter behaves obvious non-Gaussian, non-stationary, and nonlinear characteristics at a low incident angle. In recent decades, a number of approaches have been reported for ship detection in SAR images. Most methods use statistical modeling to detect patterns in SAR image data. Among them, constant false alarm rate (CFAR) detectors and their improvement methods are widely used in SAR targets detection [2]. In [3], a density censoring operation is used to identify background clutter superpixels with high densities before the CFAR detection. In order to reduce the adverse effect of outliers, a censored harmonic averaging CFAR detector is proposed in [4]. [5] proposes a CFAR detector based on bilateral trimmed statistics. [6] presents an adaptive superpixel-based CFAR detector for inshore dense ship detection in SAR image. [7] proposes an automatic-identification-system (AIS) data aided CFAR detector for multiple-target detection in SAR image. Considering the capture effect from interfering outliers which can result in the performance degradation of the CFAR detector, [8] explores a statistical indicator analysis of the impacts of the complex signal kurtosis on the decision of truncation depth to guarantee the true clutter samples. In [9], the ship detection performance of different CFAR models is analyzed and compared by the indicators of CFAR target detection loss and efficiency. The accuracy achieved with the above techniques is high but still not satisfactory, thus making detection technology an ongoing and open research subject. Statistics detection methods, looking like spending more time and effort in order to extract features or patterns, present more advantages rather than experimenting with different combinations or settings for CFAR models. In [10], a saliency detection method based on local and global contrast is proposed by exploring the different scattering mechanisms between ship targets and background clutter. [11] proposes a detection method of ship in SAR image based on two-dimensional singularity power spectrum. [12] presents a method for ship detection in high-resolution SAR images by clustering spatially enhanced pixel descriptor. [13] proposes a superpixel-based detector to improve the performance of detection by using the local contrast of fisher vectors. In [14], a superpixel-based Fisher vector is proposed to characterize the difference between the ship-target and background-clutter superpixels. [15] proposes a Fisher-vector-based adaptive superpixel segmentation algorithm of SAR image. [16] presents a method of ship detection in SAR image by using a hybrid polarimetric covariance matrix. In [17], a saliency-based filtering algorithm is proposed to filter out interference information. [18] explores the scattering feature of ships in the image domain and low rank feature in the transforming domain. [19] proposes a multisize inference fusion framework to eliminate false alarms of ship detection in large-scale SAR images. [20] presents a segmentation method for SAR images based on density-based simple linear iterative clustering. [21] proposes an automatic sea-ice classification method that integrates spatial contexture with textural features. Each feature pattern is a valued research subject both in basic theory and practical application and has its benefits and drawbacks. In designing and implementing feature pattern, care needs to be taken with the type of SAR imagery to which it is applied. Patterns designed for one type of imagery

* Corresponding author: Meng Yang (yangmeng@hdu.edu.cn).

may not be appropriate or may need to be adjusted for a different type of imagery. It is hoped that the variety of contributions shows the richness of the subject and provides new insight and perspectives. It is also believed that the SAR image feature representation of the future will be an active interplay of different groups of methods and ideas [22].

This article aims to investigate the Ricci curvatures and Finsler metric space, and the use case of these geometric structures in the detection of ship targets in SAR imagery. Ricci curvature is defined to be the trace of the Riemann curvature on each tangent space. It is a geometrical method for the study of relative chaotic behavior of close geodesics, which plays an important role in the geometry of Riemann manifolds. Finsler geometry is closely related to the calculus of variations [23]. The geometrical data in Finsler geometry consists of a smoothly varying family of Minkowski norm (one on each tangent space), rather than a family of inner products. This family of Minkowski norms is known as a Finsler structure. The Finsler manifolds form a much larger class than the Riemann manifolds.

Compared with the existing research, this innovative work mainly manifests itself in the following two aspects: it proposes the thought of Ricci-curvature representation in ship detection of SAR images; it also provides a feasible and efficient method to study Finsler metrics with certain geometric properties, which are used to improve contrast between target and background in SAR imagery.

2. PROPOSED METHODS

2.1. Ricci Curvatures

The probability density function for the Gamma distribution of intensity imagery is [24]

$$p\left(x;\gamma,\kappa\right)=\left(\frac{\kappa}{\gamma}\right)^{\kappa}\frac{x^{\kappa-1}}{\Gamma\left(\kappa\right)}\exp\left(-\frac{\kappa x}{\gamma}\right),\quad x>0 \tag{1}$$

where Γ denotes the Gamma function, γ the scale parameter, and κ the shape parameter. Set $\nu=\left(\frac{\kappa}{\gamma}\right)^{\tau}$, where τ denotes the scale modulation factor. Then the probability density functions have the form

$$f\left(x;\nu,\kappa\right)=\nu^{\kappa}\frac{x^{\kappa-1}}{\Gamma\left(\kappa\right)}\exp\left(-\nu x\right),\quad x>0 \tag{2}$$

The logarithm of Gamma density function can be written as

$$\begin{aligned}\log f\left(x;\nu,\kappa\right) &= -\left[\log\Gamma\left(\kappa\right)-\kappa\log\nu\right]\\ &\quad+\left[\kappa\log x-\nu x\right]-\log x\end{aligned} \tag{3}$$

Let $\theta=(\theta_1,\theta_2)=(\nu,\kappa)$ be a coordinate system. The potential function is defined as

$$\phi\left(\theta\right)=\phi\left(\theta_1,\theta_2\right)=\phi\left(\nu,\kappa\right)=\log\Gamma\left(\kappa\right)-\kappa\log\nu \tag{4}$$

The Fisher matrix is obtained by

$$\left[\frac{\partial^2}{\partial\theta_i\partial\theta_j}\phi\left(\theta\right)\right]=\begin{bmatrix}\kappa\nu^{-2} & -\nu^{-1}\\ -\nu^{-1} & \frac{d^2}{d\kappa^2}\log\Gamma\left(\kappa\right)\end{bmatrix} \tag{5}$$

which is a Riemann metric on the Gamma manifold based on the family of Gamma density functions. The connection coefficients $\{\Gamma^i_{jk}\}$ of the torsion-free affine connection in Riemann manifold are given by

$$\Gamma^i_{jk}=\frac{1}{2}\frac{\partial}{\partial\theta_i}\frac{\partial}{\partial\theta_j}\frac{\partial}{\partial\theta_k}\phi\left(\theta\right) \tag{6}$$

Based on the calculation and analysis, the curvature tensor expression of Gamma manifold under the special symmetric metric is given by

$$R^l_{ijk}=\frac{\partial}{\partial\theta_i}\Gamma^l_{jk}-\frac{\partial}{\partial\theta_j}\Gamma^l_{ik}+\sum_r\left(\Gamma^r_{jk}\Gamma^l_{ir}-\Gamma^r_{ik}\Gamma^l_{jr}\right) \tag{7}$$

By contraction, we obtain the Ricci tensor

$$\left[R_{ij}\right]=\begin{bmatrix}\frac{\kappa\left[\kappa\psi''(\kappa)+\psi'(\kappa)\right]}{4\nu^2\left[\kappa\psi'(\kappa)-1\right]^2} & -\frac{\kappa\psi''(\kappa)+\psi'(\kappa)}{4\nu\left[\kappa\psi'(\kappa)-1\right]^2}\\ -\frac{\kappa\psi''(\kappa)+\psi'(\kappa)}{4\nu\left[\kappa\psi'(\kappa)-1\right]^2} & \frac{\psi'(\kappa)\left[\kappa\psi''(\kappa)+\psi'(\kappa)\right]}{4\left[\kappa\psi'(\kappa)-1\right]^2}\end{bmatrix} \tag{8}$$

where $\psi'(\kappa)$ denotes $\frac{d}{d\kappa}\log\Gamma(\kappa)$, and $\psi''(\kappa)$ denotes $\frac{d^2}{d\kappa^2}\log\Gamma(\kappa)$.

2.2. Finsler Structure

Define on the Gamma manifold a metric g by

$$g=\left[g_{ij}\right]=\operatorname{sgn}\left(\left\|R_{ij}\right\|\right)\left[R_{ij}\right] \tag{9}$$

where sgn denotes the sign function, and $\|R_{ij}\|$ is the determinant of $[R_{ij}]$. According to the Finsler geometry theory, any Randers metric $F=\alpha+\beta$ can be determined by a Riemannian metric g and a vector field $V=\sum_i v^i\frac{\partial}{\partial\theta_i}$ by means of the navigation. F can be expressed by

$$\begin{aligned}F &= \frac{\sqrt{\left(1-\sum_{ij}g_{ij}v^iv^j\right)\left(\sum_{ij}g_{ij}y^iy^j\right)+\left(\sum_{ij}g_{ij}v^jy^i\right)^2}}{1-\sum_{ij}g_{ij}v^iv^j}\\ &\quad-\frac{\sum_{ij}g_{ij}v^jy^i}{1-\sum_{ij}g_{ij}v^iv^j}\end{aligned} \tag{10}$$

where $y=\sum_i y^i\frac{\partial}{\partial\theta_i}$. For the Finsler metric F, θ could stand for the statistical property of image pixels, and y is the displacement vector from the state θ to a new state.

2.3. Detection Algorithm for Ships

According to the Ricci tensors and Finsler metrics, combining the one-class support vector machine (OC-SVM), the detection procedure of ship targets in SAR images is as follows.

(1) The model parameters γ and κ are estimated by means of maximum likelihood estimation (MLE) based on pixels in moving window;

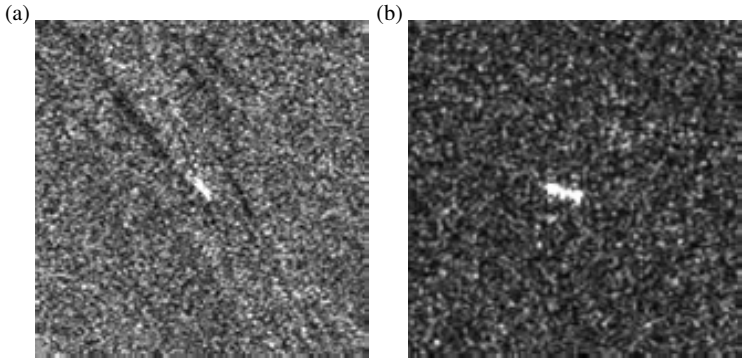

FIGURE 1. Original SAR images. (a) SAR image. (b) SAR image.

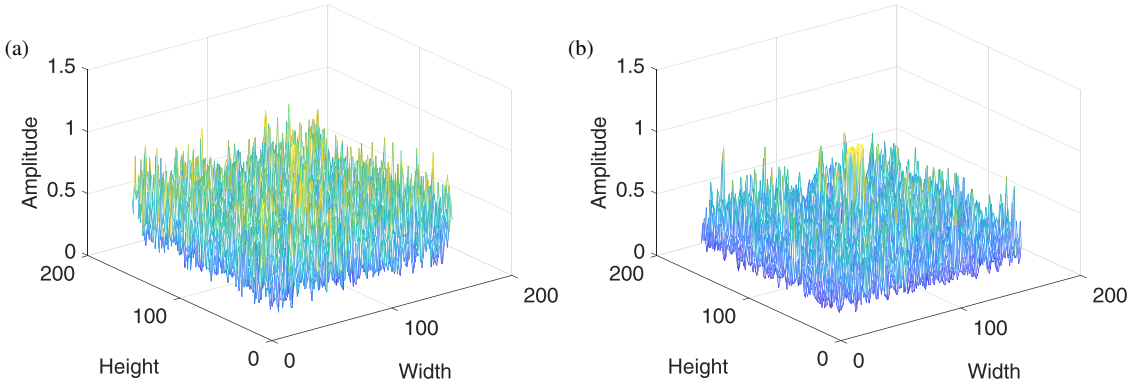

FIGURE 2. 3D plot of the image shown in Fig. 1.

(2) According to the theory derivation results, Ricci tensors $[R_{ij}]$ are calculated with formula when the parameters $\theta = (\theta_1, \theta_2) = (\nu, \kappa)$ are estimated;

(3) Set $\left(\upsilon^1, \upsilon^2\right) = \left(\nu\left(\nu^2+\kappa^2\right)^{-\frac{1}{2}}, \kappa\left(\nu^2+\kappa^2\right)^{-\frac{1}{2}}\right)$ and $\left(y^1, y^2\right) = \left(-\nu\left(\nu^2+\kappa^2\right)^{-\frac{1}{2}}, \kappa\left(\nu^2+\kappa^2\right)^{-\frac{1}{2}}\right)$. The Finsler metrics F are calculated with respect to the parameters θ;

(4) The Gamma-based CFAR detector is used to achieve a coarse detection. That is, the background and the potential target are divided in adaptive threshold module;

(5) According to the CFAR detection results, the clutter feature values F are separated. The features F of clutter data are used on the OC-SVM classifier learning and training [25];

(6) The designed anomaly detection system based on OC-SVM is used to extract outlier values (corresponding to the target) from the feature values F of SAR image.

3. EXPERIMENTAL RESULTS AND ANALYSIS

In order to show the validity of the proposed method, two SAR images (as shown in Fig. 1 and Fig. 2) are used in the experiments. According to coherent field imaging principle, speckle is only noise-like rather than an actual noise process, which degrades the SAR image quality. For the existence of strong speckle noise in SAR images, good detection results cannot be obtained with traditional methods. Most traditional detection methods are based on modelling the background statistically and then finding potential targets whose pixel values are statistically unusual. In practice, modelling ship targets and taking their statistics into account is generally too difficult owing to the factors that come into play, such as imaging scattering characteristics, radar system parameters, and SAR geometric features.

In the proposed algorithm, the first stage is to estimate the shape and scale parameters (κ, γ) based on the sliding-window and MLE techniques. The Finsler metrics F of pixels in SAR image are calculated with respect to the estimated parameters. Set $\tau = 4$. Figs. 3(a) and (b) show the Finsler metrics for pixels that show target-background differences in the high contrast.

In process detecting, the detection module extracts features from each sliced image at first and then locates the position of ships by using OC-SVM classifier with radially-gaussian kernel. To get the clutter pixels and training sample labels for OC-SVM, a CFAR detector based on Gamma distribution is used for fast pixel labeling in SAR images. As shown in Figs. 4(a) and (b), the outputs are two binary image with pixel values 0 and 1.

The final detection results are obtained by using the trained OC-SVM classifier [25]. As shown in Figs. 5(a) and (b), the proposed method is able to provide desirable detection results for SAR images. According to modern geometric theory, the curvature tensor measures noncommutativity of the covariant derivative. The Ricci curvature tensor is defined as the con-

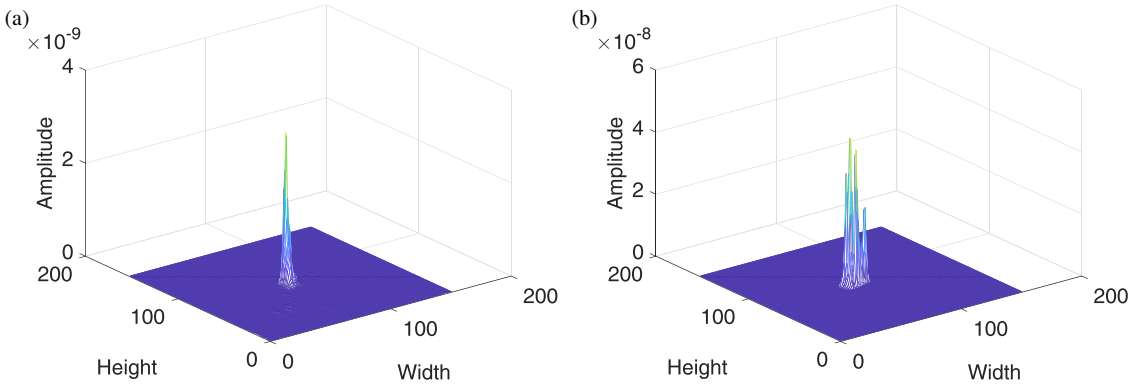

FIGURE 3. Values F of pixels.

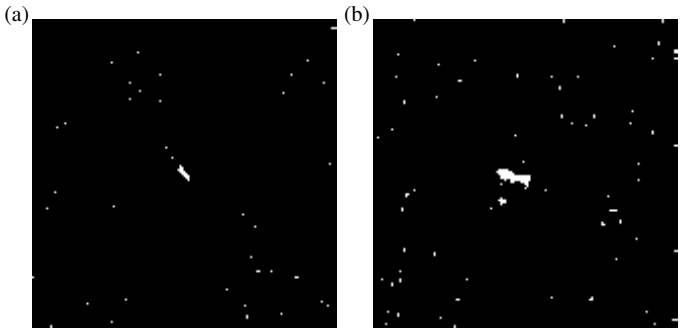

FIGURE 4. CFAR detector based on Gamma distribution for ship detection in SAR images.

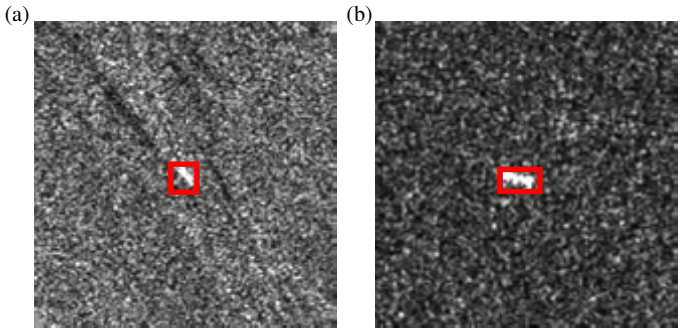

FIGURE 5. Ship detection results for SAR images.

TABLE 1. Comparison of performance for four methods.

Index	Proposed method	Lognormal-Metric [27]	Geometric-Optimization [28]	Double-parameter CFAR
DR	84.63%	85.13%	84.78%	88.86%
FAR	3.89%	4.59%	6.24%	67.43%

traction of the first and third indices of the Riemann tensor and has advantages in robustness to speckle noise.

More to the question of robustness and efficiency of the proposed method, the performance of several algorithms are validated by using GaoFen-3 PolSAR data [26]. GaoFen-3 SAR datasets, which are developed independently by China, can be downloaded by researchers through open channels. In experiments, quality factors are used to evaluate the performance of the algorithms in a quantitative way, which are defined as $DR = TP(TP + FN)^{-1}$ and $FAR = FP(TP + FP)^{-1}$, where FP denotes the false positive (false alarms), DR the detection rate, FAR the false alarm rate, FN the false negative (missing targets), and TP the true positive (detected targets). The experiments are conducted on 1000 SAR images which do not contain any land areas. The sliding window size is 9×9 and $\tau = 4$. Set CFAR detection parameters: the background-band of 25×25 pixels, guard-band of 15×15 pixels, and constant false alarm rate 10^{-9}. Table 1 shows the test results, which suggest that the proposed method has good robustness and effectiveness.

4. CONCLUSIONS

The core idea of the proposed method is to explore the different topologies of the pattern between ships and sea clutter, which are measured by Ricci curvatures and Finsler metrics. In this work, the curvature feature is first generated by calculating the Ricci tensors in a moving window. Then Finsler metric is used to represent the energy one needs in order to move from the pattern to the neighboring pattern. The analyse and experiment prove the validity of the algorithm.

The Ricci flow is a powerful technique that integrates geometry, topology, and analysis. The variety of contributions has shown the richness of the subject and provides new insight and perspectives. While research on the application of Rcci flow has taken place in mathematics and physics, the new study in this work is the first to look at the issue in the ship detection in SAR images. This article aims to find an entry point, identify a gap, and then find method doable to fill that gap. It is believed that the studies of the future will be an active interplay of different groups of methods and ideas.

ACKNOWLEDGEMENT

This work was supported by the Open Grant of State Key Laboratory of Complex Electromagnetic Environment Effects on Electronics and Information Systems (CEMEE) under Grant [CEMEE2018Z0203B]; the Zhejiang Province Science and Technology Plan Project under Grant [LGG18F010009].

REFERENCES

[1] Gao, G., *Characterization of SAR Clutter and Its Applications to Land and Ocean Observations*, Springer, 2019.

[2] Liu, T., Z. Yang, A. Marino, G. Gao, and J. Yang, "Robust CFAR detector based on truncated statistics for polarimetric synthetic aperture radar," *IEEE Transactions on Geoscience and Remote Sensing*, Vol. 58, No. 9, 6731–6747, 2020.

[3] Wang, X., G. Li, X.-P. Zhang, and Y. He, "A fast CFAR algorithm based on density-censoring operation for ship detection in SAR images," *IEEE Signal Processing Letters*, Vol. 28, 1085–1089, 2021.

[4] Zefreh, R. G., M. R. Taban, M. M. Naghsh, and S. Gazor, "Robust CFAR detector based on censored harmonic averaging in heterogeneous clutter," *IEEE Transactions on Aerospace and Electronic Systems*, Vol. 57, No. 3, 1956–1963, Jun. 2021.

[5] Ai, J., Y. Mao, Q. Luo, M. Xing, K. Jiang, L. Jia, and X. Yang, "Robust CFAR ship detector based on bilateral-trimmed-statistics of complex ocean scenes in SAR imagery: A closed-form solution," *IEEE Transactions on Aerospace and Electronic Systems*, Vol. 57, No. 3, 1872–1890, Jun. 2021.

[6] Li, M.-D., X.-C. Cui, and S.-W. Chen, "Adaptive superpixel-level CFAR detector for SAR inshore dense ship detection," *IEEE Geoscience and Remote Sensing Letters*, Vol. 19, 4010405, 2022.

[7] Ai, J., Z. Pei, B. Yao, Z. Wang, and M. Xing, "AIS data aided Rayleigh CFAR ship detection algorithm of multiple-target environment in SAR images," *IEEE Transactions on Aerospace and Electronic Systems*, Vol. 58, No. 2, 1266–1282, Apr. 2022.

[8] Li, T., D. Peng, and S. Shi, "Outlier-robust superpixel-level CFAR detector with truncated clutter for single look complex SAR images," *IEEE Journal of Selected Topics in Applied Earth Observations and Remote Sensing*, Vol. 15, 5261–5274, Jun. 2022.

[9] Gao, S. and H. Liu, "Performance comparison of statistical models for characterizing sea clutter and ship CFAR detection in SAR images," *IEEE Journal of Selected Topics in Applied Earth Observations and Remote Sensing*, Vol. 15, 7414–7430, 2022.

[10] Cui, X.-C., Y. Su, and S.-W. Chen, "A saliency detector for polarimetric SAR ship detection using similarity test," *IEEE Journal of Selected Topics in Applied Earth Observations and Remote Sensing*, Vol. 12, No. 9, 3423–3433, Sep. 2019.

[11] Xiong, G., F. Wang, L. Zhu, J. Li, and W. Yu, "SAR target detection in complex scene based on 2-D singularity power spectrum analysis," *IEEE Transactions on Geoscience and Remote Sensing*, Vol. 57, No. 12, 9993–10 003, Dec. 2019.

[12] Lang, H., Y. Xi, and X. Zhang, "Ship detection in high-resolution SAR images by clustering spatially enhanced pixel descriptor," *IEEE Transactions on Geoscience and Remote Sensing*, Vol. 57, No. 8, 5407–5423, Aug. 2019.

[13] Wang, X., G. Li, X.-P. Zhang, and Y. He, "Ship detection in SAR images via local contrast of Fisher vectors," *IEEE Transactions on Geoscience and Remote Sensing*, Vol. 58, No. 9, 6467–6479, Sep. 2020.

[14] Lin, H., H. Chen, K. Jin, L. Zeng, and J. Yang, "Ship detection with superpixel-level Fisher vector in high-resolution SAR images," *IEEE Geoscience and Remote Sensing Letters*, Vol. 17, No. 2, 247–251, Feb. 2020.

[15] Wang, X., Y. He, G. Li, and A. Plaza, "Adaptive superpixel segmentation of marine SAR images by aggregating Fisher vectors," *IEEE Journal of Selected Topics in Applied Earth Observations and Remote Sensing*, Vol. 14, 2058–2069, 2021.

[16] Zhang, T., W. Wang, Z. Yang, J. Yin, and J. Yang, "Ship detection from PolSAR imagery using the hybrid polarimetric covariance matrix," *IEEE Geoscience and Remote Sensing Letters*, Vol. 18, No. 9, 1575–1579, Sep. 2021.

[17] Zhang, P., H. Luo, M. Ju, M. He, Z. Chang, and B. Hui, "Brain-inspired fast saliency-based filtering algorithm for ship detection in high-resolution SAR images," *IEEE Transactions on Geoscience and Remote Sensing*, Vol. 60, 5201709 2022.

[18] Lv, Z., J. Lu, Q. Wang, Z. Guo, and N. Li, "ESP-LRSMD: A two-step detector for ship detection using SLC SAR imagery," *IEEE Transactions on Geoscience and Remote Sensing*, Vol. 60, 5233516 2022.

[19] Zhang, C., C. Yang, K. Cheng, N. Guan, H. Dong, and B. Deng, "MSIF: Multisize inference fusion-based false alarm elimination for ship detection in large-scale SAR images," *IEEE Transactions on Geoscience and Remote Sensing*, Vol. 60, 5224811, 2022.

[20] Wang, X., G. Li, A. Plaza, and Y. He, "Revisiting SLIC: Fast superpixel segmentation of marine SAR images using density features," *IEEE Transactions on Geoscience and Remote Sensing*, Vol. 60, 5221818, 2022.

[21] Jiang, M., D. A. Clausi, and L. Xu, "Sea-ice mapping of RADARSAT-2 imagery by integrating spatial contexture with textural features," *IEEE Journal of Selected Topics in Applied Earth Observations and Remote Sensing*, Vol. 15, 7964–7977, 2022.

[22] Bao, D., S.-S. Chern, and Z. Shen, *An Introduction to Riemann-Finsler Geometry*, Springer, 2000.

[23] Shen, Y.-B. and Z. Shen, *Introduction to Modern Finsler Geometry*, Science Press, 2013.

[24] Forbes, C., M. Evans, N. Hastings, and B. Peacock, *Statistical Distributions*, John Wiley & Sons, 2010.

[25] Ji, Y. and H. Lee, "Event-based anomaly detection using a one-class SVM for a hybrid electric vehicle," *IEEE Transactions on Vehicular Technology*, Vol. 71, No. 6, 6032–6043, Jun. 2022.

[26] Sun, X., Z. Wang, Y. Sun, W. Diao, Y. Zhang, and K. Fu, "AIR-SARShip-1.0: High-resolution SAR ship detection dataset," *Journal of Radars*, Vol. 8, No. 6, 852–862, 2019.

[27] Yang, M. and C. Guo, "Ship detection in SAR images based on lognormal ρ-metric," *IEEE Geoscience and Remote Sensing Letters*, Vol. 15, No. 9, 1372–1376, Sep. 2018.

[28] Yang, M., D. Pei, N. Ying, and C. Guo, "An information-geometric optimization method for ship detection in SAR images," *IEEE Geoscience and Remote Sensing Letters*, Vol. 19, 4005305, 2022.